Effect of Aspect Ratio on Heat Transfer in a Differentially Heated Square Cavity Using Copper-Water Nanofluid

Krishanu Sarkar[a] and Apurba Kumar Santra[b*]
[a]Department of Mechanical Engineering, National Institue Of Technology, Durgapur, India
[b]Department of Power Engineering, Jadavpur University, Salt Lake Campus, Block – LB, Plot-8, Sector – III, Salt Lake, Kolkata – 700 098, India

ABSTRACT

Effect of aspect ratio (*AR*) on heat transfer due to laminar natural convection of Cu-water nanofluid in a two-dimensional differentially heated enclosure has been studied numerically. The transport equations have been discretized using finite volume approach and solved using SIMPLER algorithm. Considering the nanofluid to be incompressible and non-Newtonian, the shear stresses have been calculated using Ostwald-de Waele model. The thermal conductivity of the nanofluid has been calculated from the proposed model by Chon *et al*. Study has been conducted for AR = 0.125 to 3 while Rayleigh number (Ra) has been varied between 10^4 and 10^7 and solid volume fraction (ϕ) of copper particles (diameter = 25 nm) varied from 0.05% to 5%. In general heat transfer decreases with increase in AR and ϕ but increases with increase in Ra. For $Ra = 10^7$, maximum heat transfer is obtained between AR = 0.15 – 0.25.

Keywords: Nanofluid; Heat transfer; Non-Newtonian, Natural Convection; Square Cavity

NOMENCLATURE

AR	Aspect Ratio (l/h)
c	specific heat (J/kg K)
d	diameter
Gr	Grashoff number
g	acceleration due to gravity (m/s^2)
H, L	dimensionless cavity height and dimensionless width of cavity
h, l	dimensional (m) height and width of cavity
k	thermal conductivity (W/mK)
k_b	Boltzmann constant
k_{eff}	effective thermal conductivity
l_f	mean free path of water
m, n	the respective consistency and fluid behaviour index parameters,
Nu_y	local Nusselt number of the heater
$\overline{Nu}$	average Nusselt number at the heater
P	pressure (N/m^2)

*Corresponding author. aksantra@pe.jusl.ac.in; Ph: +91 33 2335 5813/ 5215; Fax: +91 33 2335 7254

p	dimensionless pressure $(p–p_0)H^2/\rho_0\alpha^2$
Pr	Prandtl number of fluid, $v_f/\ \alpha_f$
Ra	Rayleigh Number, $Gr\ Pr$
Re	Reynolds number
T	temperature (K)
T_H, T_C	temperature (K) of the heat source and sink respectively
u, v	velocity components in the x and y directions respectively (m/s)
U, V	dimensionless velocities ($U = uH/\alpha$, $V = vH/\alpha$)
x, y	horizontal and vertical coordinates respectively (m)
X, Y	dimensionless horizontal and vertical coordinates respectively ($X = x/h$, $Y = y/h$)

GREEK SYMBOLS

α	thermal diffusivity of the fluid (m^2/s)
β	isobaric expansion coefficient (K^{-1})
ϕ	solid volume fraction
μ	dynamic viscosity ($N.s/m^2$)
ν	kinematic viscosity (m^2/s)
ρ	density of the fluid (kg/m^3)
θ	dimensionless temperature $(T - T_0)/\ (T_H - T_C)$
ψ	dimensionless stream function
τ	the stress tensor
$\dot{\gamma}$	the symmetric rate of deformation tensor

SUBSCRIPTS

app	apparent
eff	effective
f	fluid
nf	nanofluid
0	at reference state
p	particle
s	solid

1. INTRODUCTION

Performance of conventional fluids like water, Ethylene Glycol (EG) is limited due to their lower thermal conductivity. Nanofluid, which is a suspension of solid nanoparticles of metals and their oxides (1–100 nm diameter) in conventional liquids, has been considered as a better option due to their improved thermal conductivity [1, 2, 3]. Such enhancement depends on shape, size, concentration and thermal properties of the solid nanoparticles. The nanofluid is stable [4], introduce very little pressure drop and it can pass through nano-channels. Sometimes stabilizer is added to the nanofluid to stabilize the solid particles in the mixture [5].

Several models have been proposed by researchers to predict the effective thermal conductivity of nanofluid [6, 7, 8, 9, 10, 11], which was proved to be not realistic as the experimental values were much higher than the predicted values. However the models proposed by some researchers [12, 13, 14] considering the localized Brownian movement of nanoparticles were proved to be realistic. In these cases a constant appears that can be calculated from the experimental results. Chon *et al*. [15] have provided a correlation based on experimental results, which gives quite accurate value of effective thermal conductivity of Al_2O_3-water nanofluid. Several researchers have tried to explain the physics behind the increase in thermal conductivity [16, 17]. Buongiorno [17] have theoretically studied seven slip mechanisms that produce a relative motion between the nanoparticles and the base fluid. They have found that only Brownian motion and thermophoresis are important slip mechanism, which takes part in the enhancement in abnormal convective heat transfer of nanofluid. However, Kebliniski *et al*. [18] have

confirmed that heat transfer due to brownian motion is too slow to transport significant amount of heat through a nanofluid. This has been confirmed through analysis through MD simulation.

Revealing the rheology of nanofluid is a complicated issue. The well-known viscosity model given by Brinkman [19] gives lower value than that observed by experiments. Kwak and Kim [20] have shown experimentally that the viscosity of nanofluid depends on shear rate and zero shear viscosity increases rapidly when ϕ exceeds 0.2%. Shear thinning behaviour nanofluid has been observed by many researchers [21, 22]. They have observed that the viscosity of nanofluid increases with the increase in concentration for a given shear rate.

A few experiments have been conducted to study natural convective heat transfer using nanofluid inside a cavity [23, 24, 25]. The general observation of these experiments is that the heat transfer decreases with increase in concentration of nanoparticles in the nanofluid. This was in contrary to their expectation but it was reveled that increase in viscosity at low shear rate is the reason behind this. Recently Wen and Ding [25] have experimentally observed that for natural convection the convective heat transfer coefficient decreases with the increase in concentration of nanoparticles. They have also shown that viscosity of this nanofluid increases rapidly with the inclusion of nanoparticles as shear rate decreases. A large number of literature is found regarding natural convection with nanofluid inside a cavity. Khanafer *et al.* [26] have numerically shown that heat transfer increases with the increase in nanoparticle concentration for a particular Grashoff number for copper nanofluid in a square cavity. They had used Wasp model [7] for thermal conductivity. Their observations were contrary to the experimental result as they had considered the fluid to be Newtonian. They had considered the thermal dispersion but that involves an empirical constant, which is still unknown. Recently Santra *et al*. [27] have considered the nanofluid as non-Newtonian and have shown that heat transfer decreases with increase in particle concentration for a differentially heated square cavity. This result matches with the experimental observations. Ho *et al*. [28] showed that enhancement in the dynamic viscosity, counteracting that in the thermal conductivity of the nanofluid can thus play as a crucial factor and should be taken into account when assessing its heat transfer efficacy for natural convection in enclosures. Jou *et al.* [29] have performed the same study [26] to observe the effect of aspect ratio (AR) of the enclosure on heat transfer for Cu-water nanofluid considering ϕ upto 20%. Abunada *et al*. [30] have studied the effect of aspect ratio on heat transfer due to natural convection in a differentially heated cavity using Cu-EG-Water nanofluid. The AR was varied between 0.5 and 2. They have observed that heat transfer decreases with increase in AR.

The study on Nanofluid is promising for nanotechnology based cooling applications such as MEMS, including ultrahigh thermal conductivity coolants, lubricants, hydraulic fluids and metal cutting fluids. Since under normal condition the natural convection is the only mode of heat transfer, the components may be more prone to damage.

The present paper shows the effect of aspect ratio on heat transfer and flow pattern due to laminar natural convection of copper-water nanofluid in a differentially heated square cavity. The nanofluid has been treated as non-Newtonian. Here the single phase model has been considered so the slip has not been taken into account. In the present case the temperature difference between the hot and the cold walls are less so accordingly the effect of Brownian diffusion and thermophoresis which are the main reasons behind the slip mechanism, is less. [17]. The thermal conductivity model proposed by Chon *et al.* [15] has been used to determine the effective thermal conductivity (k_{eff}) of the nanofluid. The viscosity of nanofluid has been calculated using Ostwald-de Waele model (two parameter power law model) for a non-Newtonian shear thinning fluid [27]. Santra *et al*. [27] had used copper particles for their study. Hence in the present study Cu-water nanofluid has been considered. Since the nanofluid is stable the effect of sedimentation is any has not been considered in the present study.

To the best of the knowledge of the authors, no other numerical study on buoyancy driven heat transfer analysis using nanofluid particularly considering the fluid as non-Newtonian and the aforesaid thermal conductivity model has been reported so far. Here the authors have used the primitive variables, instead of stream function & vorticity method [26, 29].

2. MATHEMATICAL FORMULATION

2.1. Problem statement

The geometry of the present problem is shown in Figure 1. It consists of a two-dimensional square enclosure of height h and width l. The temperatures of the two sidewalls of the cavity are maintained at T_H and T_C, where T_C has been considered as the reference condition. The top and the bottom horizontal walls have been considered to be insulated *i.e.*, non-conducting and impermeable to mass transfer. The enclosure is filled with a mixture of water and solid spherical copper particles of 25 nm diameter. The nanoparticles are of uniform shape and size. The nanofluid is assumed to be non-Newtonian, incompressible and the flow is laminar. Also it is assumed that the liquid and solid are in thermal equilibrium and they flow at same velocity. All the thermophysical properties are kept constant except the density, which has been incorporated only in the body force term by employing the Boussinesq approximation.

2.2. Governing equations and boundary conditions

The continuity, momentum and energy equations for a steady, two-dimensional flow of a Fourier constant property fluid have been considered. The governing equations for a steady, two-dimensional flow are as follows

$$\frac{\partial u}{\partial x}+\frac{\partial v}{\partial y}=0., \tag{1}$$

$$\rho_{nf,o}\left(u\frac{\partial u}{\partial x}+v\frac{\partial u}{\partial y}\right)=-\frac{\partial p}{\partial x}-\left[\frac{\partial \tau_{xx}}{\partial x}+\frac{\partial \tau_{yx}}{\partial y}\right] \tag{2}$$

$$\rho_{nf,o}\left(u\frac{\partial v}{\partial x}+v\frac{\partial v}{\partial y}\right)=-\frac{\partial p}{\partial y}+\left[\phi\rho_{s,o}\beta_s+(1-\phi)\rho_{f,o}\beta_f\right]g(T-T_C)-\left[\frac{\partial \tau_{xy}}{\partial x}+\frac{\partial \tau_{yy}}{\partial y}\right] \tag{3}$$

$$u\frac{\partial T}{\partial x}+v\frac{\partial T}{\partial y}=\alpha_{nf}\left[\frac{\partial^2 T}{\partial x^2}+\frac{\partial^2 T}{\partial y^2}\right] \tag{4}$$

$$\text{where,}\quad \alpha_{nf}=\frac{k_{nf}}{(\rho Cp)_{nf,o}} \tag{5}$$

where the relationships between the shear stress and shear rate in case of two-dimensional motion in rectangular co-ordinate according to the Ostwald-de Waele model are as follows: [31]

$$\tau=-m\left[\left|\sqrt{\frac{1}{2}(\dot{\gamma}\cdot\dot{\gamma})}\right|^{(n-1)}\right]\dot{\gamma} \tag{6}$$

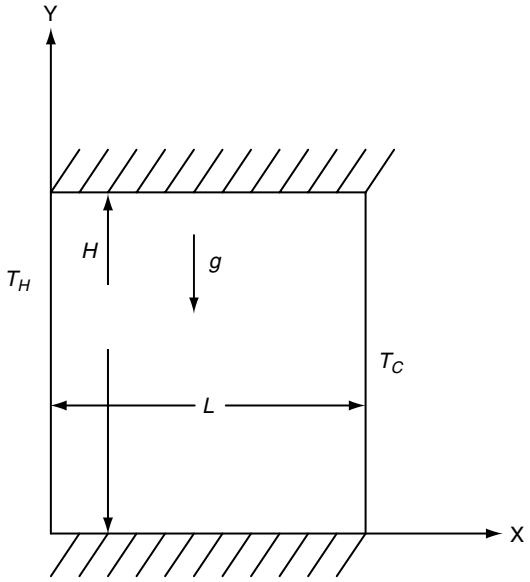

Figure 1. Geometry of the present proble.

where
$$\frac{1}{2}(\dot{\gamma}\cdot\dot{\gamma}) = 2\left\{\left(\frac{\partial u}{\partial x}\right)^2 + \left(\frac{\partial v}{\partial y}\right)^2\right\} + \left(\frac{\partial v}{\partial x} + \frac{\partial u}{\partial y}\right)^2 \tag{7}$$

Thus the stress tensors of the equations (2) and (3) take the following forms

$$\tau_{xx} = -2\left\{m\left|\left[2\left\{\left(\frac{\partial u}{\partial x}\right)^2 + \left(\frac{\partial v}{\partial y}\right)^2\right\} + \left(\frac{\partial v}{\partial x} + \frac{\partial u}{\partial y}\right)^2\right]^{\frac{1}{2}}\right|^{(n-1)}\right\}\left(\frac{\partial u}{\partial x}\right) \tag{8}$$

$$\tau_{yx} = \tau_{xy} = -\left\{m\left|\left[2\left\{\left(\frac{\partial u}{\partial x}\right)^2 + \left(\frac{\partial v}{\partial y}\right)^2\right\} + \left(\frac{\partial v}{\partial x} + \frac{\partial u}{\partial y}\right)^2\right]^{\frac{1}{2}}\right|^{(n-1)}\right\}\left(\frac{\partial u}{\partial y} + \frac{\partial v}{\partial x}\right) \tag{9}$$

$$\tau_{yy} = -2\left\{m\left|\left[2\left\{\left(\frac{\partial u}{\partial x}\right)^2 + \left(\frac{\partial v}{\partial y}\right)^2\right\} + \left(\frac{\partial v}{\partial x} + \frac{\partial u}{\partial y}\right)^2\right]^{\frac{1}{2}}\right|^{(n-1)}\right\}\left(\frac{\partial v}{\partial y}\right) \tag{10}$$

Here m and n are two empirical constants, which depend on the type of nanofluid used. Putra *et al*. [24] have shown experimentally the relation between the shear stress and shear strain for Al_2O_3-water nanofluid. Using this data, the values of m and n have been calculated for 1% and 4% solid volume fraction. These values are suitably interpolated and extrapolated keeping in mind that the shear stress

decreases with increase in ϕ for a particular shear rate in the mixture. The values of m and n for different ϕ have been given in Table 1. It is to be noted that for a shear thinning fluid the value of n is less than 1 [31]. Since the rate of change of shear stress with shear rate for Cu-water nanofluid is not available, these data of Al_2O_3-water nanofluid has been adopted for Cu-water nanofluid to observe the nature of the heat transfer.

The effective density of the nanofluid at reference temperature is

$$\rho_{nf,0} = (1-\phi)\rho_{f,0} + \phi\rho_{s,0} \tag{11}$$

and the heat capacitance of nanofluid is

$$(\rho Cp)_{nf} = (1-\phi)(\rho Cp)_f + \phi(\rho Cp)_s \tag{12}$$

The effective thermal conductivity of fluid has been determined by the model proposed by Chon *et al.* [15]. For the two-component entity of spherical-particle suspension the model gives

$$\frac{k_{eff}}{k_f} = 1 + 64.7\varphi^{0.7460}\left(\frac{d_f}{d_p}\right)^{0.3690}\left(\frac{k_p}{k_f}\right)^{0.7476} Pr^{0.9955}\, Re^{1.2321} \tag{13}$$

Where

$$\mathrm{Re}\frac{\rho_f k_b T}{3\pi\mu^2 l_f} \tag{14}$$

Here k_b is the Boltzmann constant, value of which is 1.3807 × 10–23 J/K and l_f is the mean free path of water, the value of which is 0.17 nm [15]. The calculation of effective thermal conductivity can be obtained from equation (13).

The above equations can be converted to non-dimensional form, using the following dimensionless parameters

$$X = x/h,\ Y = y/h,\ U = uh/\alpha,\ V = vh/\alpha,\ P = (p - p_0)\cdot h^2/(\rho_{nf,0}\cdot \alpha^2) \text{ and}$$
$$\theta\,(T - T_C)/(T_H - T_C)$$

Table 1. Values of fluid behaviour index parameters (m, n).

Solid Volume Fraction (ϕ) (%)	***m* (N.sec^n.m^{-2})**	***n***
0.5	0.00187	0.880
1.0	0.00230	0.830
1.5	0.00283	0.780
2.0	0.00347	0.730
2.5	0.00426	0.680
3.0	0.00535	0.625
3.5	0.00641	0.580
4.0	0.00750	0.540
4.5	0.00876	0.500
5.0	0.01020	0.460

Then the non-dimensional equations will be as follows

$$\frac{\partial U}{\partial X}+\frac{\partial V}{\partial Y}=0, \tag{15}$$

$$U\frac{\partial U}{\partial X}+V\frac{\partial U}{\partial Y}=-\frac{\partial P}{\partial X}+\frac{\mu_{app}}{\rho_{nf,0}}\frac{}{\alpha_{f,0}}\left[\frac{\partial^2 U}{\partial X^2}+\frac{\partial^2 U}{\partial Y^2}\right] \tag{16}$$

$$U\frac{\partial V}{\partial X}+V\frac{\partial V}{\partial Y}=$$

$$-\frac{\partial P}{\partial Y}+Gr\ Pr\ Pr\frac{\rho_{f,0}}{\rho_{nf,0}}(1-\phi+\phi\frac{\rho_s\beta_s}{\rho_f\beta_f})\theta+\frac{\mu_{app}}{\rho_{nf,0}}\frac{}{\alpha_{f,0}}\left[\frac{\partial^2 V}{\partial X^2}+\frac{\partial^2 V}{\partial Y^2}\right] \tag{17}$$

$$U\frac{\partial \theta}{\partial X}+V\frac{\partial \theta}{\partial Y}=\frac{k_{nf}}{k_f}\frac{(\rho Cp)_{f,0}}{(\rho Cp)_{nf,0}}\left[\frac{\partial^2 \theta}{\partial X^2}+\frac{\partial^2 \theta}{\partial Y^2}\right] \tag{18}$$

Here the apparent viscosity of the nanofluid is

$$\mu_{app}=m\left(\frac{a_{f,0}}{h^2}\right)^{(n-1)}\left|\left[2\left\{\left(\frac{\partial U}{\partial X}\right)^2+\left(\frac{\partial V}{\partial Y}\right)^2\right\}+\left(\frac{\partial V}{\partial X}+\frac{\partial U}{\partial Y}\right)^2\right]^{\frac{1}{2}}\right|^{(n-1)} \tag{19}$$

The boundary conditions, used to solve equations (15) to (18) are as follows.

$$u=v=\frac{\partial T}{\partial y}=0 \text{ at } y=0,h \text{ and } 0\le x\le l;$$

$$\text{i.e.,} U=V=\frac{\partial \theta}{\partial Y}=0 \text{ at } \boldsymbol{Y}=0,1.0 \text{ and } 0\le X\le 1.0.$$

$$T=T_H, u=v=0 \text{ at } x=0 \text{ and } 0\le y\le h;$$

$$\text{i.e.,}\theta=1.0 \text{ and } U=V=0 \text{ at } X=0 \text{ and } 0\le Y\le 1.0.$$

$$T=T_C, u=v=0 \text{ at } x=l \text{ and } 0\le y\le h;$$

$$\text{i.e.,}\theta=0 \text{ and } U=V=0 \text{ at } X=1.0 \text{ and } \mathbf{0}\le Y\le 1.0.$$

Equations. (15) to (18), along with the boundary conditions are solved numerically. From the converged solutions, we have calculated ^{Nu}y (Local Nusselt number) and $\overline{Nu}$ (Average Nusselt number) for the hot wall as follows

$$Nu_y=-\frac{k_{eff}}{k_f}\frac{\partial \theta}{\partial X}\Big|_{X=0,Y} \tag{20}$$

$$\overline{Nu} = \frac{1}{H} \int_0^H Nu_y \bullet dY \Big|_{X=0} \tag{21}$$

where, H is dimensionless cavity height.

The dimensionless stream function ψ has been defined as $U = \partial\psi/\partial Y$ and $V = -\partial\psi/\partial X$. The stream function at any grid location (X,Y) is calculated as

$$\psi(X,Y) = \int_{Y_0}^{Y} U \cdot \partial Y + \psi(X, Y_0) \tag{22}$$

Along the solid boundary the stream function is taken as zero. $\psi(X, Y_0)$ is known either from the previous calculation, or, from the boundary condition.

2.3. Numerical approach and validation

The governing mass, momentum and energy equations have been dicretized by a control volume approach using a power law profile approximation. The computational domain has been divided into 81 X 81 non-uniform grids. Finer grids have been taken at the boundaries. The set of discretized equations have been solved iteratively, through alternate direction implicit ADI, using the SIMPLER algorithm [32]. For convergence, under-relaxation technique has been employed. To check the convergence, the mass residue of each control volume has been calculated and the maximum value has been used to check the convergence. The convergence criterion has been set to 10^{-7}.

The results are validated with the results of de Vahl Davis [33] for different *Ra*, which has been summarized in Table 2. The difference between the average Nusselt number of de Vahl Davis and that obtained by the present code is well within acceptable limit. Apart from this the average Nusselt number closely matches with that of Santra *et al*. [27] for $AR = 1$.

3. RESULTS AND DISCUSSION

The effect of aspect ratio (*AR*) on heat transfer due to laminar natural convection in a differentially heated enclosure has been studied numerically. Water has been considered as the base fluid with $Pr = 7.02$ (the base temperature considered here is 20°C). Solid spherical nanoparticles of copper of 25 nm diameter dispersed in water are considered to be the nanofluid. The effective thermal conductivity of the nanofluid has been calculated from the correlation given by Chon *et al*. [15]. This effective thermal conductivity depends on temperature. The thermal properties as well as the physical properties have been tabulated in Table 3. The values of the constants *m* and *n* are summarized in Table 1, to calculate the effective viscosity of the nanofluid. Results are presented for different *AR* (from 0.125 to 3) while *Ra* and ϕ have been varied from 10^4 to10^7 and from 0.0 % to 5.0% (with the increment of 0.5%) respectively. The temperature of the hotter wall is 40°C (313 K) and that of the cold wall is 20°C (293 K).

Table 2. Comparison of results for validation.

Rayleigh Number (*Ra*)	$\overline{Nu}$ of de Vahl Davis	$\overline{Nu}$ of present code
10^4	2.243	2.245
10^5	4.519	4.521
10^6	8.799	8.813

Table 3. Thermophysical properties of different phase at 20°C.

Property	Fluid (water)	Solid (copper)
C_p (J/Kg K)	4181.80	383.1
ρ(Kg/m^3)	1000.52	8954.0
k(W/m K)	0.597	386.0
β(K^{-1})	210.0×10^{-6}	51.0×10^{-6}

3.1. Effect of aspect ratio on streamlines and isotherms

Since the heat transfer depends on the flow pattern and the temperature variation within the cavity, the effect of *AR* on the streamlines and the isotherms has been shown.

Figure 2 represents the streamlines and isotherms for $Ra = 10^7$ for different *AR* when $\phi = 5\%$. From the obtained diagrams of streamlines it is observed that the dimension of the central cavity of the circulation is increasing with the increase in *AR* as well as the thickness of the velocity boundary layer is increasing. It is observed from the figures of streamlines that the maximum value of dimensionless stream function is increasing with the increase in the *AR* at a very slow rate. The maximum value becomes 19 when the *AR* is 1 and this value remains to be constant for the *AR* 2 and 3. This observation indicates that the velocity of flow has a tendency to increase with the increase in *AR*.

The diagrams of isotherms show that the density of isotherms changes when the *AR* is altered. For lower values of *AR* the isotherms are closely placed and the spacing between isotherms increases with the increase in *AR*. Also the thickness of the thermal boundary layer is increasing and the isothermal stagnant core is also increasing. This is due to the fact that with the increase in *AR*, the width of the cavity is increasing. Therefore fluid has to travel a longer distance so the tendency of heat transfer by convection reduces. Thus the probability of heat transfer by conduction increases.

The obtained patterns of isotherms and streamlines hint at the presence of immobile fluid particles at the centre of the cavity.

Figure 3 depicts the streamlines and isotherms for $\phi = 0\%$ to 5% when $Ra = 10^7$ and $AR = 0.75$. It is observed that the strength of the circulation decreases with the increase in concentration of the nanoparticles in the suspension. The figures of streamlines at the same time show that the dimension of the core zone is decreasing with the increase in solid volume fraction. As the nanofluid is non-Newtonian its viscosity enhances with the increase in nanoparticle concentration. As a result of which the velocity of the nanofluid reduces thus increasing the velocity boundary layer thickness. According to the figures of isotherms it is evident that the isotherms are closely place at lower values of nanoparticle concentration in the suspension. The density of the isotherms is decreasing with the increase in concentration of the nanoparticles in the suspension. As the nanofluid is non-Newtonian the viscosity increases with the increase in ϕ therefore the velocity of the particles reduces. So diffusion increases with increase in ϕ causing increase in thermal boundary layer thickness.

3.2. Effect of solid volume fraction on average Nusselt number

The average Nusselt number for various *AR* and ϕ has been presented in Fig. 4 for $Ra = 10^7$.

The figure shows that for a particular ϕ the average Nusselt number first increases with increase in *AR* and after achieving an optimum value it decreases gradually. This peak value shifts towards right with increase in nanoparticle concentration. The maximum heat transfer is observed between $AR = 0.15$ to 0.25. As *AR* increases from 0.15, the space available for molecular movement increases, at the same time the dimension of the central core increases, these two factors play the major role in defining the optimum *AR* for heat transfer. At $AR = 0.15$ the circulation is suppressed as the space for fluid movement is limited. As *AR* increases this space increases and convection as well as heat transfer increases. After reaching the optimum value, it decreases again as the boundary layer thickness increases with increase in *AR* as described in Figure 2.

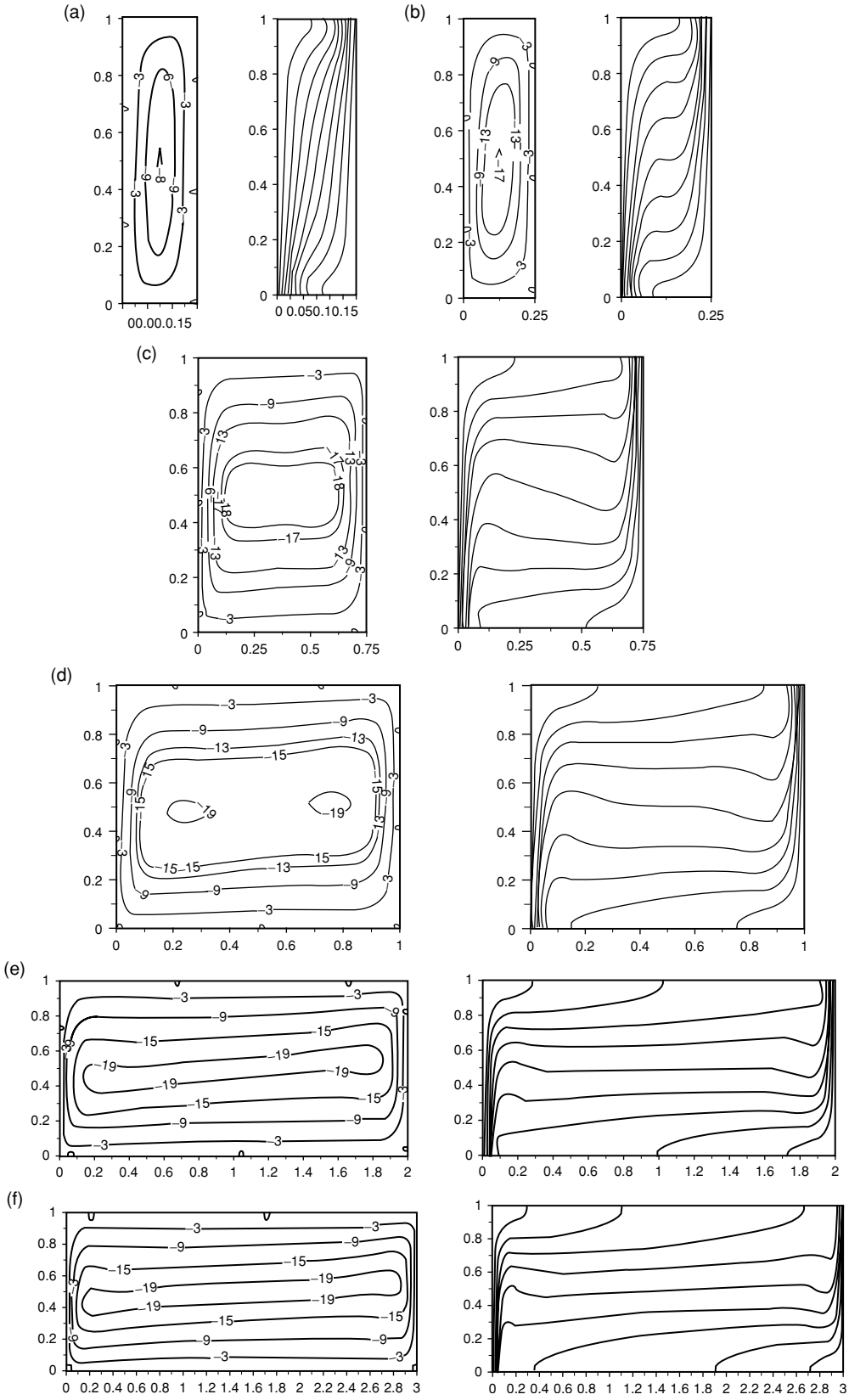

Figure 2. Streamlines and isotherms for $Ra = 10^7$, ϕ=5% for AR = (a) 0.15, (b) 0.25, (c) 0.75, (d) 1.0, (e) 2.0 and (f) 3.0.

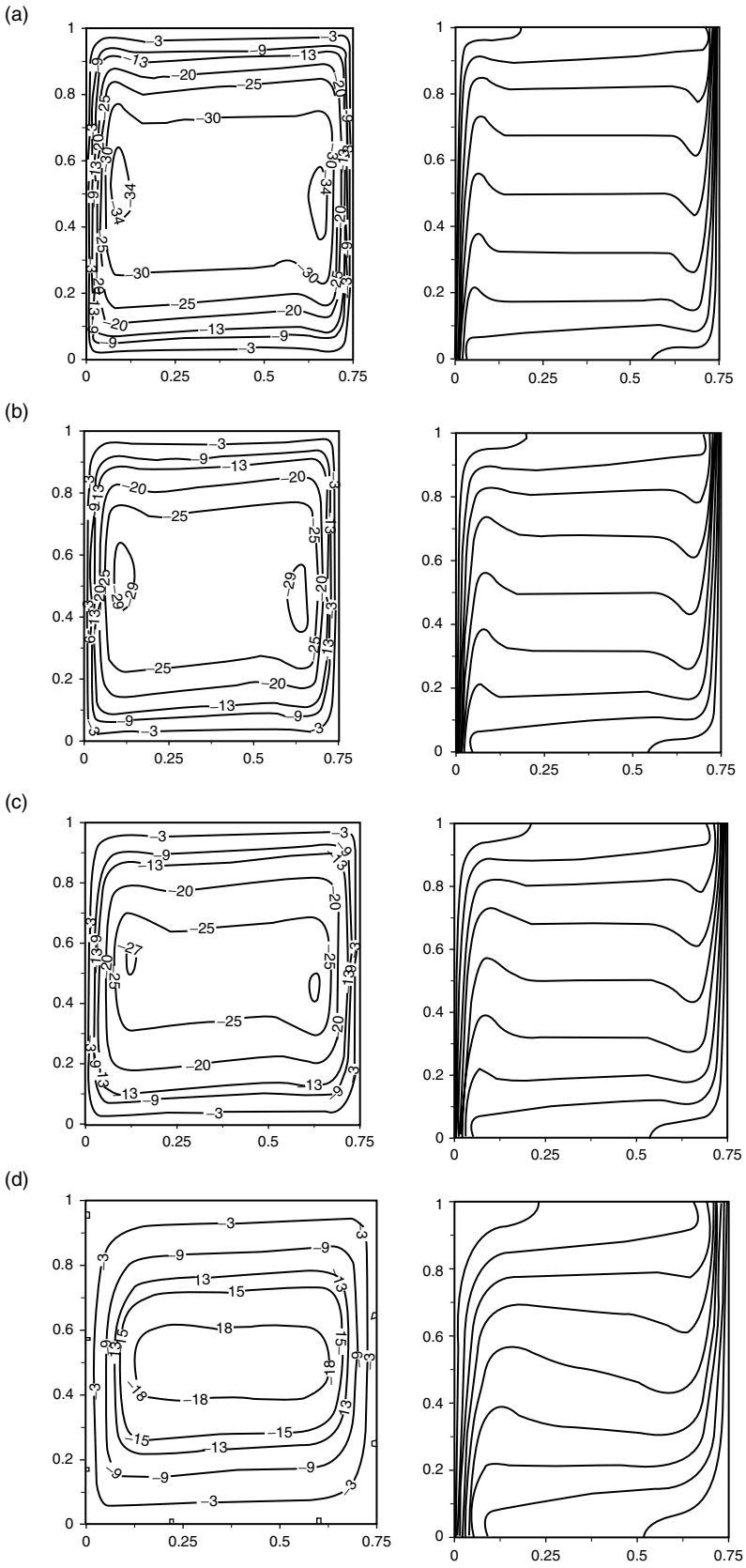

Figure 3. Streamlines and isotherms for $Ra = 10^7$, AR 0.75 for ϕ = a) 0%, b) 1%, c) 2%, d) 5%.

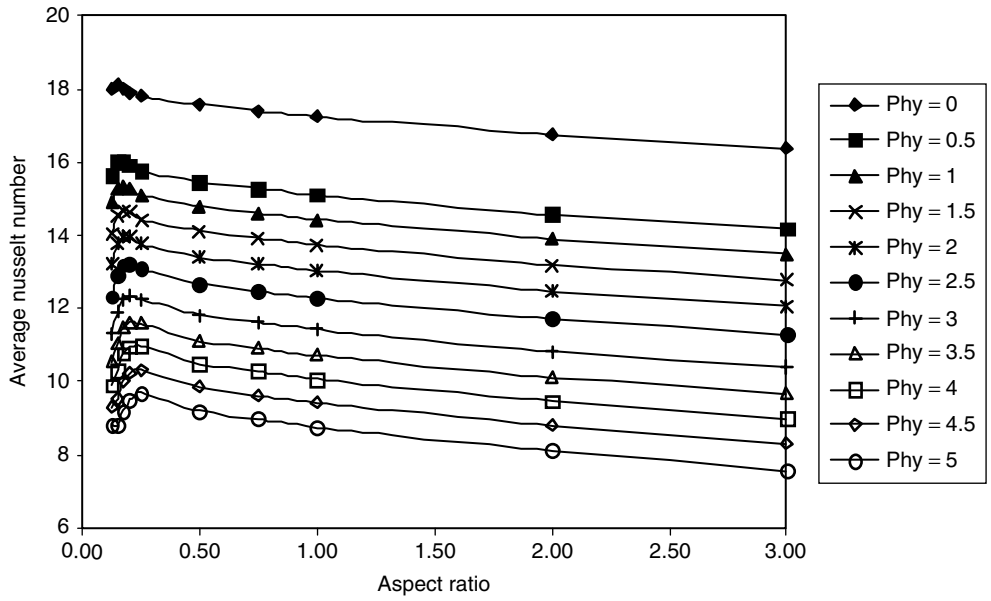

Figure 4. Variation of average Nusselt number with Aspect Ratio and ϕ for Ra=10^7.

It is also observed that the average Nusselt number decreases for a particular AR with increase in ϕ. It is apparent that the heat transfer should increase with ϕ as effective thermal conductivity of nanofluid increases with ϕ . But here we observe the opposite phenomena as the fluid is non-Newtonian and shows shear-thinning behaviour. Hence the viscosity increases with ϕ , which decrease the convective heat transfer. This can also be explained from Figure 3. As with increase in ϕ the thermal boundary layer thickness increases, the heat transfer decreases. Thus increase in heat transfer due to conduction is nullified. Such observations are similar to the various experimental result [24, 25].

Figure 5 shows the variation of heat transfer with *AR* for different *Ra* when $\phi = 5\%$. It shows that as the *Ra* decreases from 10^7, the heat transfer decreases initially at a higher rate, which becomes sluggish eventually. This is due to the fact that effect of viscosity dominates over convection at lower *Ra*, as strength of circulation reduces with decrease in Rayleigh number. Figure 6 shows the result of

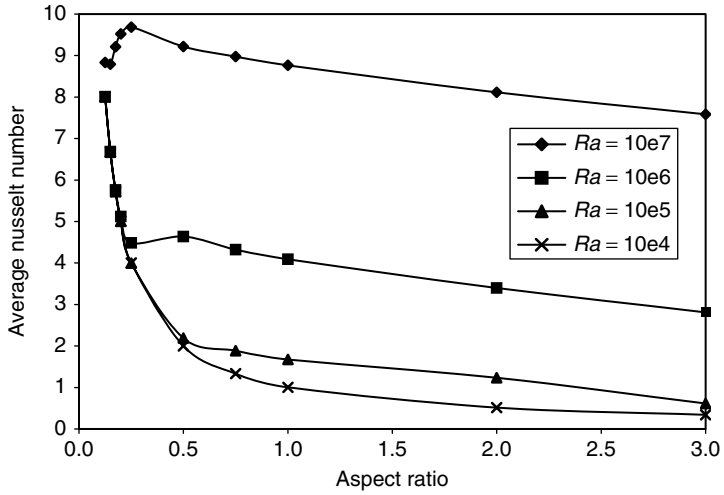

Figure 5. Variation of average Nusselt number with Aspect Ratio and *Ra* for ϕ=5%.

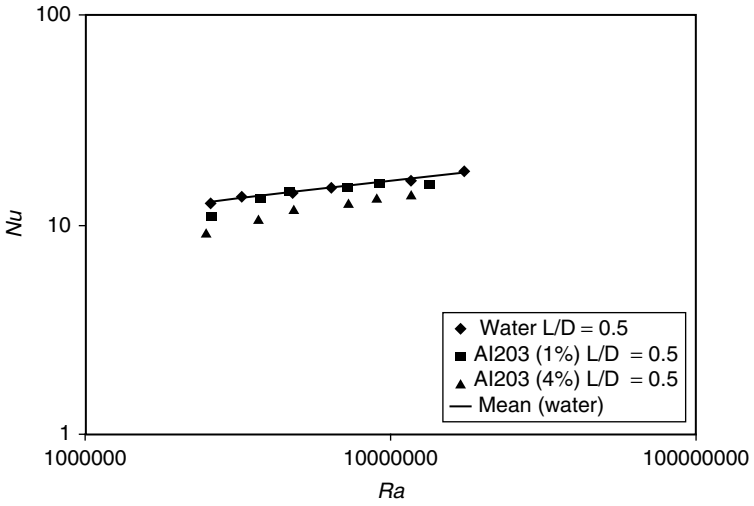

Figure 6. Result of Putra *et al.* [24].

Putra *et al*. [24] for comparison with the present result. It is observed that for every Rayleigh no the heat transfer decreases when solid volume fraction of Alumina increases from 1– 4%. Comparing the graph of putra et al with that of present study it is observed for $Ra = 10^7$ and solid volume fraction 1% the value of average Nusselt number is almost similar. Thus the numerical model gives quite reasonable value of heat transfer which almost matches with the experimental result available.

4. CONCLUSIONS

In a differentially heated enclosure the effect of aspect ratio (*AR*) on heat transfer has been numerically studied where Cu-water nanofluid has been considered. The Rayleigh number and solid volume fraction have been varied from 10^4–10^7 and 0%–5% respectively. The range of *AR* used in this case is from 0.125 to 3. The nanofluid used consists of copper nanoparticles suspended in pure water. The Prandtl number of water has been considered 7.02 and diameter of copper nanoparticles is 25 nm. The hot wall and the cold wall are kept at 40°C and 20°C respectively. The nanofluid exhibits non-Newtonian nature. Shear stress has been calculated using Ostwald-de Waele model. The effective thermal conductivity has been calculated using the model propsed by Chon *et al*.

The results show that the heat transfer decreases with increase in Aspect ratio for a particular solid volume fraction and Rayleigh Number. The trend is slightly different for $Ra = 10^7$, where heat transfer first increases and then decreases. For a particular ϕ, the highest value of heat transfer has been observed for $Ra = 10^7$, $AR = 0.15$–0.25.

Experiments should be carried out for observing the nature of heat transfer in this type of differentially heated cavities.

REFERENCE

[1] Lee S., Choi S.U.S., Li S. and Eastman J. A., Measuring Thermal Conductivity of Fluids Containing Oxide Nanoparticles, Trans ASME J. of Heat Transfer, 121, (1999) 280–289.

2] Eastman J.A., Choi S.U.S., Li S., Yu W. and Thompson L. J., Anomalously Increased Effective Thermal Conductivities of Ethylene Glycol-Based Nanofluids Containing Copper Nanoparticles, Applied Physics Letter, 78, (2001) 718–720.

[3] Xuan Y. and Li Q., Heat Transfer Enhancement of Nanofluids, Int. J. Heat and Fluid Flow, 21, (2000) 5–64.

[4] Zhou D.W., Heat Transfer Enhancement of Copper Nanofluid with Acoustic Cavitation, Int. J. Heat and Mass Transfer, 47, (2004) 3109–3117.

[5] Patel H.E., Das S. K., Sundarrajan T., Nair A. S., George B. and Pradeep T., Thermal conductivities of naked and monolayer protected metal nanoparticle based nanofluids: Manifestation of anomalous enhancement and chemical effects, Applied Physics Letters, 83 (2003) 2931–2933.

[6] Hamilton R.L. and Crosser, O.K., Thermal conductivity of heterogeneous two-component systems, I & EC Fundamentals 1, (1962) 182–191.

[7] Wasp F.J., Solid-Liquid Flow Slurry Pipeline Transportation. Trans. Tech. Pub., Berlin. (1977).

[8] Maxwell-Garnett J.C., Colours in metal glasses and in metallic films, Philos. Trans. Roy. Soc. A 203, (1904) 385–420.

[9] Bruggeman D.A.G., Berechnung Verschiedener Physikalischer Konstanten von Heterogenen Substanzen, I. Dielektrizitatskonstanten und Leitfahigkeiten der Mischkorper aus Isotropen Substanzen. Annalen der Physik. Leipzig 24 (1935) 636–679.

[10] Wang B. X., Zhou L.P. and Peng X. F., A Fractal Model for Predicting the Effective Thermal Conductivity of Liquid with Suspension of Nanoparticles, Int. J. Heat and Mass Transfer, 46, (2003) 2665–2672.

[11] Yu W. and Choi S.U.S., the role of interfacial layer in the enhanced thermal conductivity of nanofluids: A renovated Maxwell model, Journal of Nanoparticles Research, (2003) 167–171.

[12] Kumar D. H., Patel H. E., Kumar V. R. R., Sundararajan T., Pradeep T. and Das S. K., Model for conduction in nanofluids, Physical Review Letters, 93 (2004) 144301-1-3.

[13] Prasher R., Bhattacharya P and Phelan P. E., Brownian-Motion-Based Convective-Conductive Model for the Effective thermal Conductivity of Nanofluid, ASME Journal of Heat Tranfer, 128 (2006) 588–595.

[14] Patel H.E., Sundarrajan T, Pradeep T., Dasgupta A., Dasgupta N. and Das S. K., A micro-convection model for thermal conductivity of nanofluid, Pramana-journal of Physics, 65 (2005) 863–869.

[15] Chon et al APPLIED PHYSICS LETTERS 87, 153107 _2005_ .

[16] Xuan Y. and Roetzel W., Conceptions for Heat Transfer Correlation of Nanofluids, Int. J. Heat and Mass Transfer, 43, (2000) 3701–3707.

[17] Buongiorno J., Convective transport in nanofluids, Journal of Heat Transfer, 128 (2006) 240–250.

[18] Keblinski P., Phillpot S. R., Choi S.U.S. and Eastman J. A., Mechanisms of Heat Flow in Suspensions of Nano-sized Particles (Nanofluids), Int. J. Heat and Mass Transfer, 45, (2002) 855–863.

[19] Brinkman H.C., The Viscosity of concentrated suspensions and solutions, J. Chemistry Physics, 20 (1952) 571–581.

[20] Kwak K. and Kim C., Viscosity and thermal conductivity of copper oxide nanofluid dispersed in ethylene glycol, Korea-Australia Rheology Journal, 17 (2005) 35–40.

[21] Chang H, Jwo C. S., Lo C. H., Tsung T. T., Kao M. J. and Lin H. M., Rheology of CuO nanoparticle suspension prepared by ASNSS, Rev. Adv. Material Science 10 (2005) 128–132.

[22] Ding Y., Alias H., Wen D. and Williams R. A., Heat transfer of aqueous suspensions of carbon nanotubes ((CNT nanofluids), Int. J. Heat and Mass Transfer, 49 (2006) 240–250.

[23] Kang C., Okada M., Hattori A. and Oyama K., Natural convection of water-fine particle suspension in a rectangular vessel heated and cooled from opposing vertical walls (classification of the natural convection in the case of suspension with narrow-size distribution), Int. J. Heat Mass Transfer, 44 (2001) 2973–2982.

[24] Putra N., Roetzel W. and Das S.K., Natural convection of nano-fluids, Heat and Mass Transfer, 39 (2003) 775–784.

[25] Wen D. and Ding Y., Natural Convective Heat Transfer of Suspensions of Titanium Dioxide Nanoparticles (Nanofluids), IEEE TRANSACTIONS ON NANOTECHNOLOGY, 5 (2006) 220–227.

[26] Khanafer K., Vafai K. and Lightstone M., Buoyancy-driven Heat Transfer Enhancement in a Two-dimensional Enclosure Utilizing Nanofluids, Int. J. Heat and Mass Transfer, 46 (2003) 3639–3653.

[27] Santra A. K., Sen S. and Chakraborty Niladri, Study of Heat Transfer Augmentation in a Differentially Heated Square Cavity Using Copper-Water Nanofluid, International Journal of thermal Sciences, 47 (2008), 1113–1122.

[28] Ho C J, Chon M W and Li Z W, Numerical simulation of natural convection of nanofluid in a square enclosure: Effects due to uncertainties of viscosity and thermal conductivity, Int. J. Heat and Mass Transfer, 51 (2008) 4506–4516.

[29] Jou R.Y. and Tzeng S. C., Numerical research of nature convective heat transfer enhancement filled with nanofluids in rectangular enclosures, International Communications in Heat and Mass Transfer, 33 (2006) 727–736.

[30] Abunada E. and Chakma A. J., Effect of nanofluid variable properties on natural convection in enclosures filled with a CuO-EG-Water nanofluid, Int. J. Thermal Sciences, 49 (2010) 2339–2352.

[31] Bird R.B., Stewert W.E. and Lightfoot E.N., Transport Phenomena, John Wiley & Sons, Singapore, 1960.

[32] Patankar S.V, Numerical Heat Transfer and Fluid Flow, Hemisphere, Washington D. C., (1980).

[33] de Vahl Davis G., Natural Convection of Air in a Square Cavity, a Benchmark Numerical Solution, Int. J. Numer. Methods Fluids, 3 (1962) 249–264.